VALUE-ADDED 5-STORY STEEL FRAME AND ITS COMPONENTS: PART 2 - FULL-SCALE TESTS OF BEAM-COLUMN-GUSSET PLATE ASSEMBLIES

Y. Ooki[1], K. Kasai[2], Y. Azuma[3], S. Motoyui[4], and K Kaneko[5]

[1] *Assistant Professor, Structural Engineering Research Center, Tokyo Institute of Technology, Yokohama. Japan*
[2] *Professor, Structural Engineering Research Center, Tokyo Institute of Technology, Yokohama. Japan*
[3] *Former Student, Dept. of Build Environment, Tokyo Institute of Technology, Yokohama. Japan*
[4] *Associate Professor, Dept. of Build Environment, Tokyo Institute of Technology, Yokohama. Japan*
[5] *Former Postdoctoral Research Fellow, Tokyo Institute of Technology, Yokohama. Japan*
Email: ooki@serc.titech.ac.jp, kasai@serc.titech.ac.jp,
motoyui@enveng.titech.ac.jp, kaneko.kensaku@obayashi.co.jp

ABSTRACT :

This paper discusses the full-size experiment of beam-column-gusset plate assemblies. High strength and high ductility are required so that the passively-controlled structure demonstrate an enough performance under a severe earthquake. However, the behavior of those assemblies has not been clarified satisfactorily and further improvement of the design method is expected. A new loading method in which a hydraulic jack is applied as a virtual damper is developed and the case of steel damper is mainly discussed. Also dampers with velocity sensitivity, such as viscoelastic damper can be tested under static condition by this method. A frame with typical members of the 5-story steel building is set as a standard specimen, and inter story drift is increased from 1/800 to 1/33. Two cycles are applied in each loading cycle. Furthermore, fatigue tests are conducted under the story drift of 1/50 or 1/33. Consequently, the effect of the presence of the gusset plate, stiffeners, and damper force on failure mode, cumulated deformation capacity, hysteretic behavior, and distribution of strain is discussed.

KEYWORDS: E-Defense, Shaking Table, Steel Frame, Subassembly Test, Full-Scale

1. INTRODUCTION

The structural characteristics of the beam, column, and gusset plate connection have large effect on the performance, such as the story stiffness and energy dissipation, of the passively-controlled structure. In order to guarantee the performance under severe earthquakes, it is important to grasp the behavior of the system including frame, damper, and connection. There are a few researches regarding the above problems. Instability of the frame with the buckling restrained brace caused by the rotation for out-plain (Inoue et al, 2002), and the effect of characteristics of the connection of buckling restrained brace on the out-plain behavior of the brace (Takeuchi et al, 2004) are discussed in Japan. Also in US, the subassembly test including the buckling restrained brace are carried out (Roeder et al, 2006). In that research, although the frame and the brace are designed according to the current design practice, some problems, such as low deformation capacity of the system aroused by the failure of the gusset plate connection, are found.

In the E-Defense project, full scale 5-story steel structure including four kinds of dampers will be tested on shaking table (Kasai et al, 2007) and is preferred to be free from damage of the frame under severe earthquake. In order to achieve the above mentioned performance, detailed examination of the beam-column-gusset plate assemblies is requested and the full-scale tests are conducted.

2. FULL-SCALE SUBASSEMBLY TESTS

2.1. Hybrid Test Combining Subassembly and Virtual Damper

The performance of passively-controlled building depends not only on damper but also on frame members and connections. In addition to the bending moment and shear caused by the story drift, relatively large axial force

develops in the elements because of the damper force. The axial force can cause earlier yielding and possibly buckling in the elements. In order to develop a design method to control such failure, full-scale tests and analyses have been conducted on subassemblies consisting of beam, column, and gusset plate, and interim results are reported here.

Figure 1 shows the concept of a simplified hybrid test method combining a subassembly and a virtual damper. The subassembly has a configuration of L-shape, and it represents a quarter portion of the frame. We define "positive loading" when the beam is in positive (tension) axial force and positive moment, and vice versa (Figure 1).

Figure 2a shows the test-set-up, where laterally supported L-shape specimen is connected to Link-1 and Link-2 that keep the distance between the midpoint of the brace and inflection points in beam and column, respectively, see Figure 1. Two parallel actuators (total 3,000 kN capacity) are used for the displacement control to satisfy the target story drift, and one actuator diagonally placed (1,000 kN capacity) for the force control simulating damper force. The target story drift is given, but target damper force depends on the change Δu_a in diagonal distance (Figure 2a). The target damper force is calculated by substituting the measured Δu_a into the mathematical model of the damper at every step of the test, and the actuator applying such a force is called the "virtual damper". The virtual damper can apply the force of any damper type, as long as the mathematical model is available. The steps for displacement control, force control, and damper force calculation are schematically shown in Figure 2b.

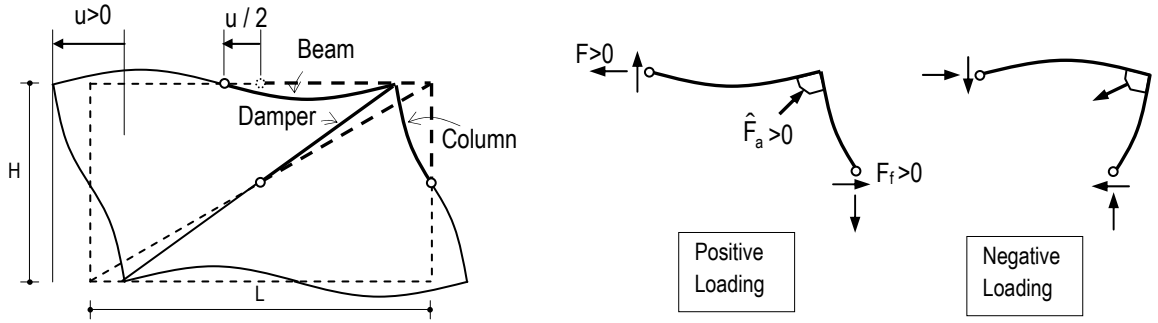

Figure 1 Concept of hybrid test and definitions of positive loading

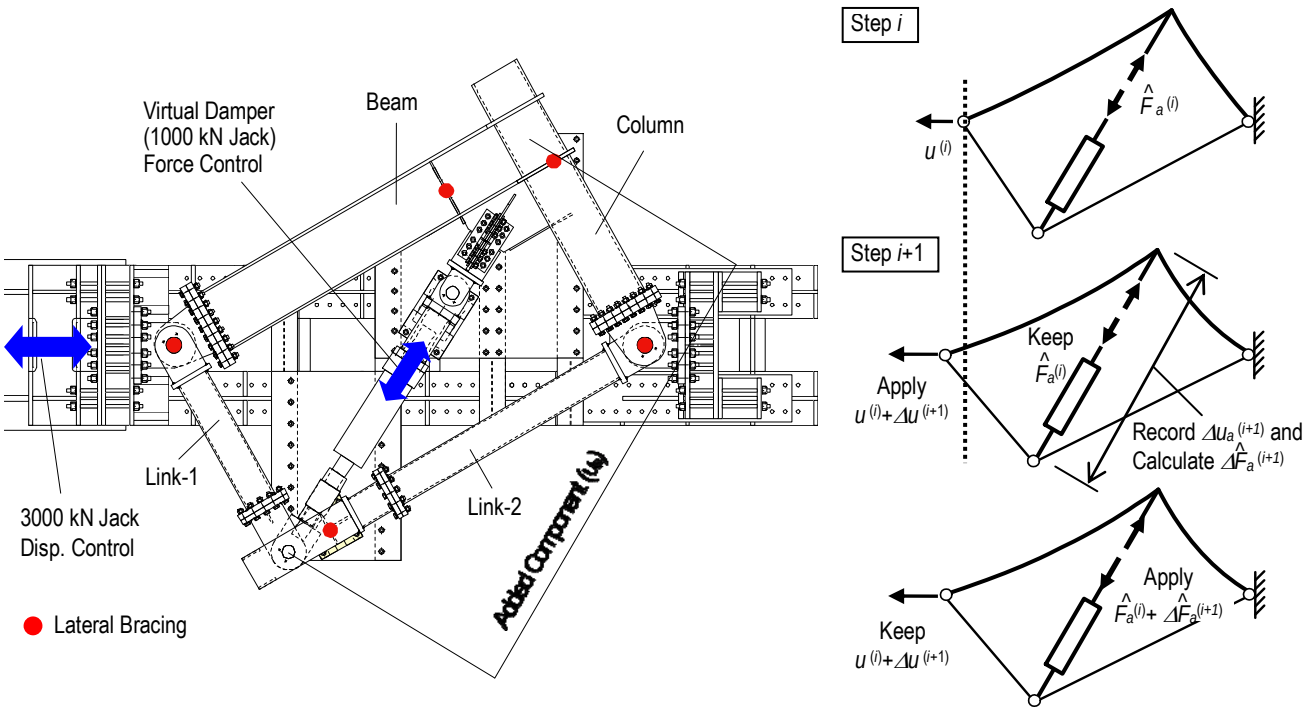

Figure 2 (a) set-up, and (b) procedure of hybrid test

Note that under the positive and negative loading cases (Figure 1), the bottom flange of the beam near the gusset tends to develop relatively large tension strain and compression strain, respectively. This is analytically illustrated in Figure 3, where possibility of local buckling under negative loading is clearly shown by our extensive nonlinear finite element analysis.

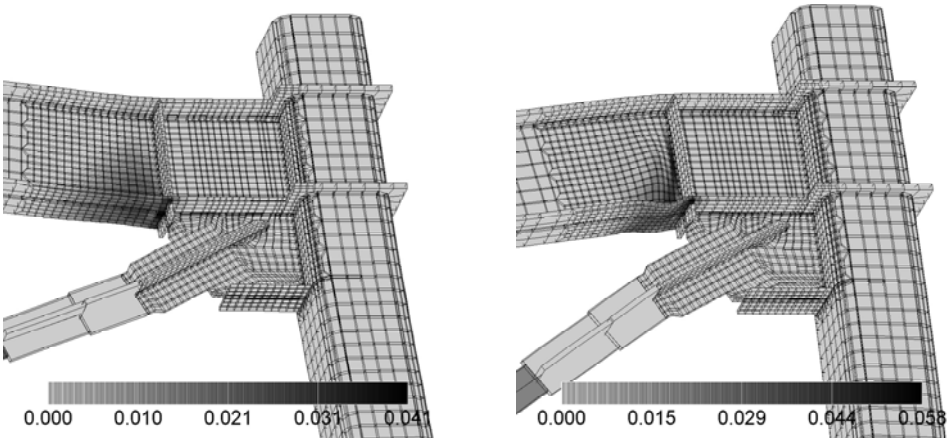

Figure 3 FEM analysis results for positive and negative loading cases

2.2. Specimens and Loading Schemes

Figure 4 shows a typical specimen. The beam is of a built-up section of 500 mm depth, 12 mm web thickness, 250 mm flange width, and 22 mm flange thickness. The column is a square box section of 400 mm × 400 mm × 19 mm. The nominal yield strength of the steel material is 325 MPa for all the elements, and actual yield stresses are 371, 357, 351, and 372 MPa for the beam web, beam flange, column, and gusset plate, respectively, unless noted. The beam satisfies the Japanese compact section requirement for a beam as well as a beam-column (Guideline 1991). The beam-column connection is a fully-restrained type.

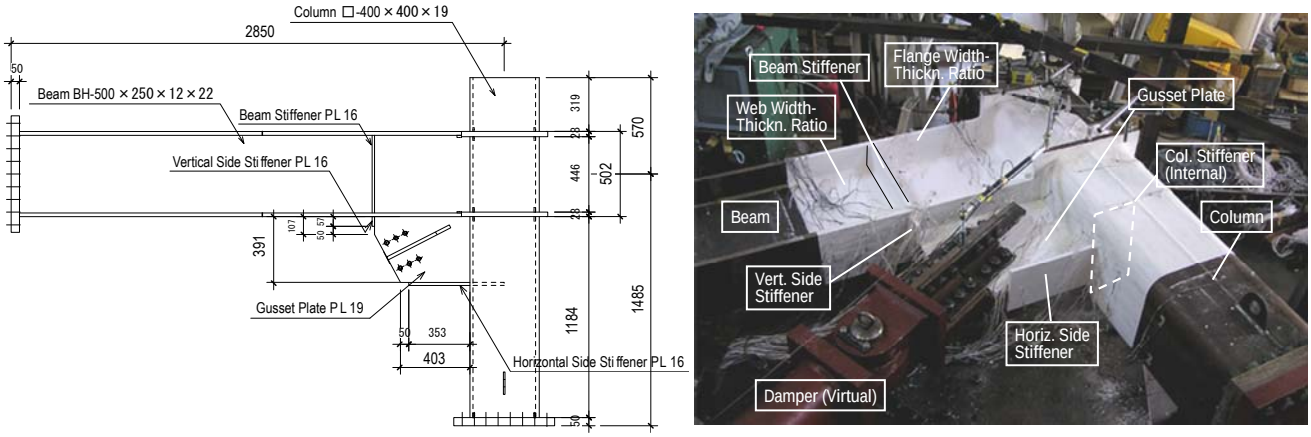

Figure 4 Typical full-scale subassembly specimen

Table 1 summarizes the specimen types. Specimen 1 has neither gusset plate nor stiffeners, and is not subjected to the damper force. Specimens 2 to 6, and 9 have a common configuration depicted by Figure 4. Specimen 2, however, is not subjected to the damper force, and only the effect of story drift is examined. Specimens 3 and 4 are benchmark specimens, meaning that they have the typical configuration (Figure 4) and are subjected to the damper force.

In specimen 5, the web is thinner (9 mm) and does not meet the Japanese code requirement for a beam-column compact section, while barely satisfying the requirement for a beam. In specimen 6, both web and flange are thinner (9 mm and 16 mm, respectively), and the flange slightly violates the compact section requirement for a beam. Specimen 7 has neither horizontal side stiffeners nor column stiffener, and specimen 8 has no stiffeners at all. Specimen 9 has a gusset plate of thickness less than 0.5 times (9 mm) the typical value of 19 mm.

All specimens are loaded with two cycles of story drift of ±1/800, ±1/400, ±1/200, ±1/100, and ±1/50 rad (0.00125, 0.0025, 0.005, 0.01, and 0.02 rad), respectively. Further, specimens 1 to 3 are loaded with multiple cycles of ±1/50 rad (0.02 rad) until failure. Specimens 4 to 9 are loaded with multiple cycles of ±1/33 rad (0.03 rad) until failure. In general, the steel (elasto-plastic, EP) damper force is considered. Exceptionally, for specimen 4, the viscoelastic (VE) damper force is considered during application of the gradually increased peak drift, and it is switched to the steel damper force during ±1/33 rad (0.03 rad).

Table 1 Specimen types and cumulative deformation capacities

No.	Specimen Type	N_f	N_f'	N_f''	θ^*
1	No Damper Force, No Gusset	111	118	120	±1/50
2	No Damper Force	123	125	126	±1/50
3	Benchmark (EP Damper / EP Damper)**	55	101	104	±1/50
4	Benchmark (VE Damper / EP Damper)***	4	8	45	±1/33
5	Large Width-Thickness Ratio for Web	0	3	24	±1/33
6	Large Width-Thickness Ratios for Web and Flange	0	0	6	±1/33
7	No Horizontal Side Stiffener, No Column Stiffener	11	22	45	±1/33
8	No Stiffeners at All	6	16	43	±1/33
9	Thin Gusset Plate	6	17	18	±1/33

* Story drift θ* indicated in this column was applied repeatedly until failure.
** EP (steel) damper force was considered for both loading cases, with gradually increased peak story drift and with constant peak story drift, respectively.
*** VE damper force was considered for loading with gradually increased peak story drift, and EP damper force considered for loading with constant peak story drift, respectively.

3. TEST RESULTS

3.1 Failure Mode

Figure 5 shows the failure modes due to multiple cycles of ±0.03 rad. Specimens 2, 3, and 7 showed failure mode 1 in Figure 5, that is, the bottom flange failed at the welded and thus heat-affected zone near the gusset plate, vertical side stiffener, and beam stiffener. Flange local buckling was less severe due to the smaller drift ±0.02 rad applied to specimens 2 and 3, as well as due to reduced deformation demand caused by the increased joint flexibility at the column tube wall and gusset plate in specimen 7. Thus, the strains are concentrated in the region immediately outside the gusset area where maximum moment develops on the beam.

Specimens 5 and 8 showed failure mode 2, where the bottom flange failed at more than 130 mm away from the gusset (Figure 5). Since local buckling is very severe in specimen 5, and since amount of welding is minimum in specimen 8, the strain concentration occurred due to localized and severe bending of the flange plate. Specimens 4, 6, and 8 showed failure mode 3, where the weld connecting the flange and web fractured due to severe local buckling of both the flange and web. Flange buckling was the most severe in specimens 4 and 6.

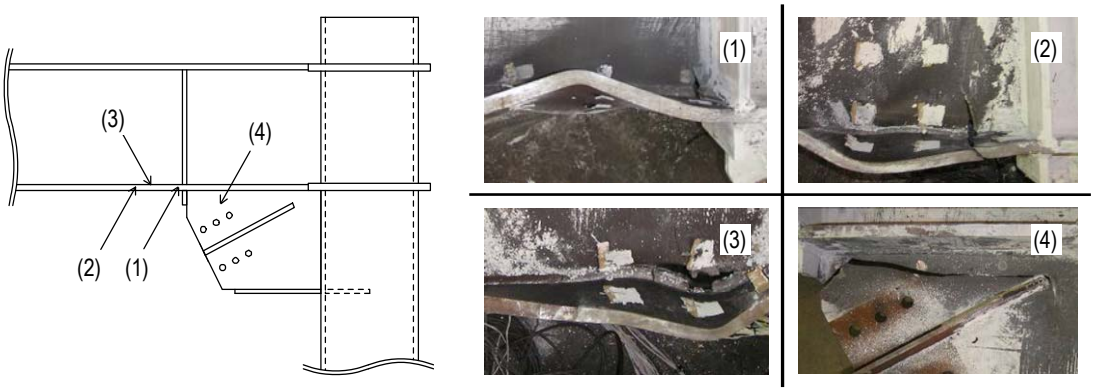

Figure 5 Various failure modes observed

Specimen 9 showed failure mode 4, where tearing of the gusset plate progressed in the horizontal direction from the edge of the vertical side stiffener and gusset plate. The strain gage records indicate large shear strains at the upper portion of the gusset, where horizontal component of the virtual damper force is transmitted to the beam. The tension force, developed along the inclined gusset edge during the positive loading, might have caused the crack initiation at the vertical side stiffener.

3.2 Cumulated Deformation Capacity

Table 1 also summarizes the numbers of cycles applied up to certain failures defined. For specimens 1 to 3, the story drift angle of ±0.02 rad is used as mentioned. For specimens 4 to 9, ±0.03 rad is used. Note that N_f, N_f', and N_f'' are the numbers of cycles where the absolute peak force becomes 0.8, 0.7, and 0.5 times the largest magnitude experienced at the earlier cycle, respectively. At cycle number N_f'', significant tearing occurred in the subassembly.

There is remarkable difference of number of cycles to the failure between the story drift angles of ±0.02 and ±0.03 rad, as seen from specimens 3 and 4. The specimens are believed to be at almost the same condition, before applying such cycles with the common EP damper force. They show more than ten-fold difference of N_f = 55 and 4, respectively (Table 1). When applying ±0.02 rad, flange local buckling was slight, and the peak force remained stable during many repeated cycles (Figure 6a). As for ±0.03 rad, the flange local buckling occurred from the first cycle, and the beam kept deteriorating at the subsequent cycles, resulting in significantly lowered peak force of the frame at the negative loading (Figure 6b).

This trend becomes more significant when the width-thickness ratios of the flange and web are large, like specimens 5 and 6 (Figure 6d). The peak forces of these specimens at negative loading case decreased to 0.8 or 0.7 times the largest peak force during application of the cyclic deformation with increasing peak drift angle, prior to application of ±0.03 rad story drift angle. Note that specimen 7 with no horizontal stiffener and no column stiffener survived much longer than the others (Figure 6c), since the beam deformation demand decreased due to the increased joint flexibility at the column tube wall and gusset plate, as mentioned earlier.

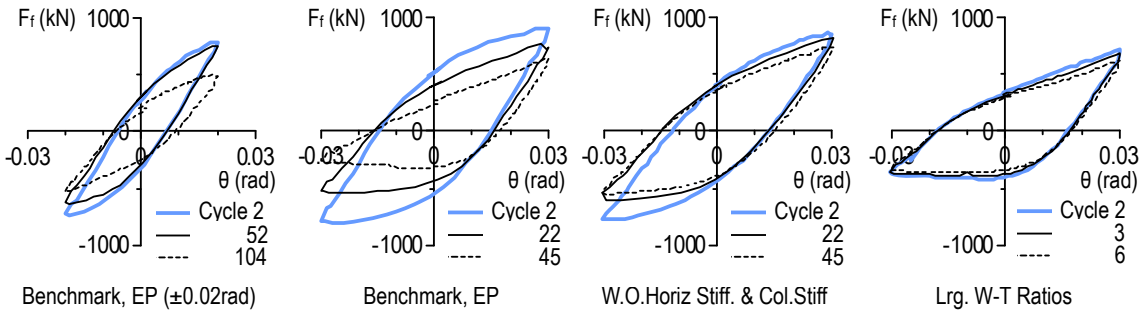

Figure 6 Frame force vs. Story drift angle (specimens 3, 4, 7, and 6 from left)

3.3 Hysteretic Behavior

In Figure 7, the horizontal forces of the system (F), frame (F_f), and damper (F_a) are plotted against the story drift angle (θ). The positive directions of the forces are already defined in Figure 1, where $\hat{F}_a$ indicates the force at an inclined brace angle.

The top row of Figure 7 shows the effect of local buckling, up to story drift of ±0.02 rad. The effect is not as great as the case of ±0.03 rad discussed earlier (Figures 12b-d)), but is still obvious from both F_f-θ and F-θ curves. Although the flange and web thicknesses are reduced by about 25%, the damper force has not changed appreciably (right figure), thus, the beam axial stress has increased by about 25%. This and moderate local buckling have caused reduction in the beam moment, and consequently horizontal force F_f of the frame. The bottom row of Figure 7 compares of effects of EP damper and VE damper. The VE damper force is larger than the EP damper force at story drift angle of ±0.02 rad. The systems combining the subassembly and these virtual dampers show clearly different hysteretic behavior, but the inelastic strains of the beams and gusset plate were similar in both cases, as can

be understood from F_f-θ curves. Note, however, that VE damper force can be larger than considered in the present study, and such a case will be investigated later by using a larger jack.

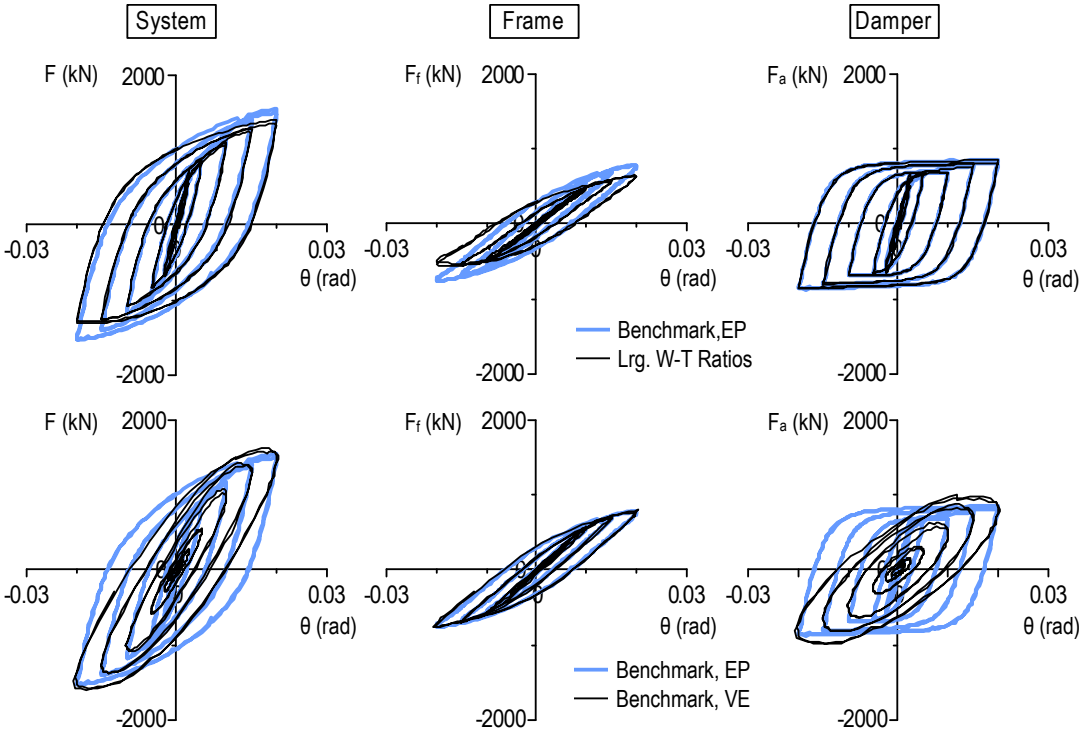

Figure 7 Forces of system, frame, and dampers with respect to story drift angle
(specimens 3 vs. 6, and specimens 3 vs. 4)

3.4 Distribution of Strain

Figure 8 shows distributions of strain around the gusset plate. In specimen 2, the damper force does not work and the direction of the shear force at the beam web which is adjacent to the gusset plate is opposite to that of specimen 1. This is caused by the gusset plate and strain at the boundary of the gusset plate concentrates on the edge of the vertical and the horizontal side stiffeners. The damper force works on specimen 3 and specimen 7, and the concentration of strain extends along the gusset plate boundary part. From the direction of the principal strain, shear strain seems to be distinguished there. On the other hand, in specimen 7, in which horizontal side stiffener and column stiffener are removed, the concentration of strain at the boundary is mitigated as compared with specimen 3. This is aroused because out-plane deformation is allowed on the column tube wall. And the distribution of strain in adjacent beam web is similar to that of specimen 1 not but specimen 2 and 3. The distribution of strain at the gusset plate of specimen 8 is almost same as that of specimen 7.

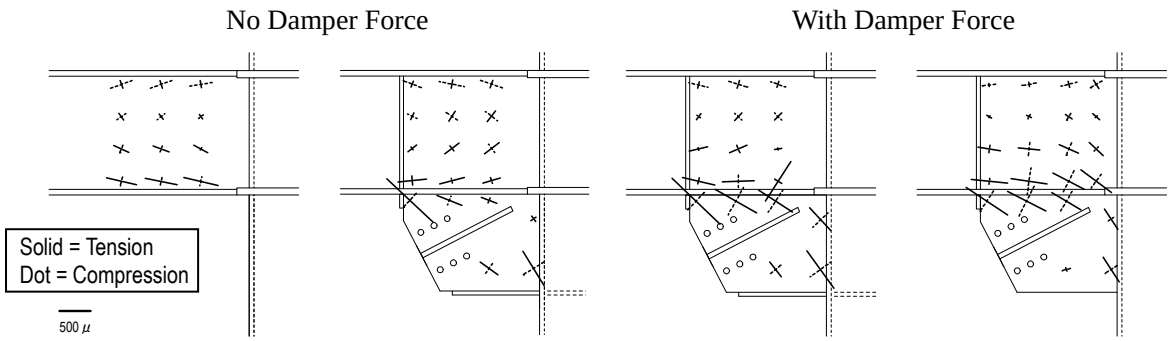

(a) Specimen 1 (b) Specimen 2 (c) Specimen 3 (with stiffener) (d) Specimen 7 (no stiffener)

Figure 8 Distribution of principal strain (story drift angle = +1/200)

For further analysis of the gusset plate, in Figure 9, normal stress and shear stress at the boundary of the gusset plate are shown which are obtained from strain gauge record. The normal stress is mainly concentrated around the vertical and the horizontal stiffener regardless of the presence of the damper force. On the contrary, shear stress is uniformly distributed along the boundary under the presence of damper force.

The concentration of stress at boundary is more significant around the bottom flange of the beam than the column tube wall and this is pointed out by Lee and Uang (2001). The design procedure considering the stress condition of gusset plate has not been proposed yet and it will be examined by means of the further experiments and analyses.

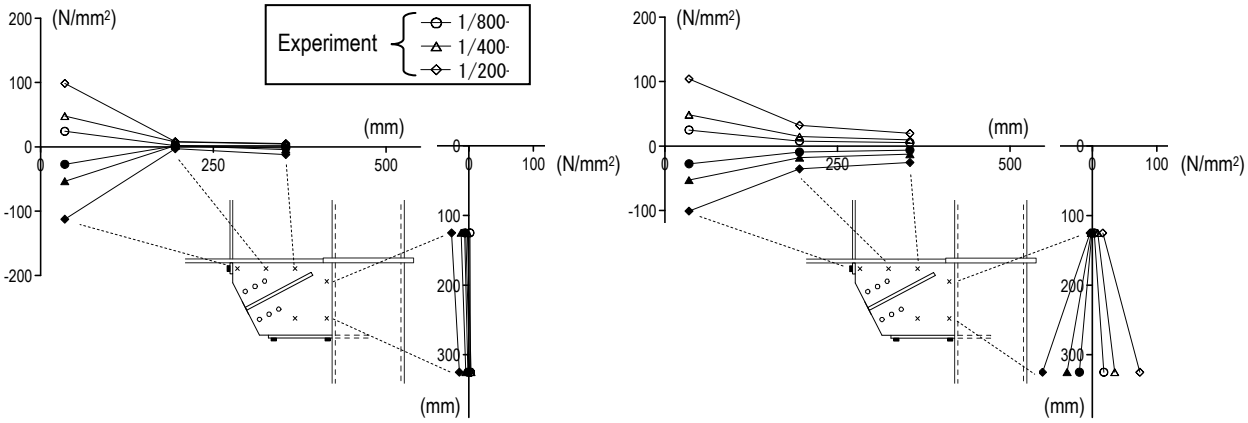

(a) Specimen 2, normal stress

(b) Specimen 2, shear stress

(c) Specimen 3, normal stress

(d) Specimen 4, shear stress

Figure 9 Distribution of normal stress and shear stress

5. CONCLUSIONS

Detailed tests and analyses have been conducted for the beam-column-gusset subassemblies with different details and thicknesses. This paper has explained interim results from such studies.

The proposed hybrid test combining subassembly and virtual damper functioned very well. Nine subassemblies were tested and four kinds of the failure modes are observed. When the flange and web thicknesses are reduced, the beam axial stress has increased and this promoted the local buckling of the flange as well as the reduction of the beam moment under ±0.02 rad loading. By the way, as for ±0.03 rad, the flange local buckling occurred from the first cycle, and the beam kept deteriorating at the subsequent cycles.

As for the cumulated deformation capacity, ten-fold difference of the number of cycles to the failure is observed between ±0.02 rad and ±0.03 rad loading. Specimen with no horizontal stiffener and no column stiffener survived

much longer than the others, since the beam deformation demand decreased due to the increased joint flexibility at the column tube wall and gusset plate.

By the proposed test method, passive control system not only with deformation dependent damper but also with velocity dependent damper can be tested in static condition. The systems with the EP and the VE damper show clearly different hysteretic behavior, but the inelastic strains of the beams and gusset plate were similar in both cases.

The concentration of stress at the boundary of the gusset plate is more significant around the bottom flange of the beam than around the column tube wall. And the normal stress is mainly transferred by the vertical and the horizontal stiffener, while the shear stress is uniformly distributed along the gusset boundaries.

REFERENCES

Inoue, K., Tembata, H., Koetaka, Y., and Uemura, K. (2002). Study on the Plane Outside Buckling of Buckling-Restrained Braces Including Joints. Summaries of Technical Papers of Annual Meeting. Architectural Institute of Japan 2002, C1, 563-564. (in Japanese)

Takeuchi, T., Yamada, S., Kitagawa, M., Suzuki, K., and Wada A. (2004). Stability of Buckling-Restrained Braces Affected by the Out-of-Plane Stiffness of the Joint Element. *Journal of Structural and Construction Engineering. Transactions of AIJ*, **575**, 121-128. (in Japanese)

Kasai, K., Ooki, Y., Motoyui S., Takeuchi T., and Sato, E. (2007). E-Defense Tests on Full-Scale Steel Buildings: Part 1 – Experiments Using Dampers and Isolators. ASCE Str. Congress, Long Beach, CA, May 16-19, 2007

Building Center of Japan (BCJ) (1991). Guidelines to Structural Calculation under the Building Standard Law. Ministry of Construction, Japan

Lee, C-H. and Uang, C-M. (2001). Analytical Modeling and Seismic Design of Steel Moment Connections with Welded Straight Haunch. *Journal of Structural Engineering*, **127:9**, 1028-1035